Journal of Medicinal Chemistry Article

J. Med. Chem. **2011,** *54,* 699–708 **699**
DOI: 10.1021/jm1010513

Identification of a Novel Scaffold for Allosteric Inhibition of Wild Type and Drug Resistant HIV-1 Reverse Transcriptase by Fragment Library Screening

Matthis Geitmann,[†] Malin Elinder,[‡] Christian Seeger,[†,‡] Peter Brandt,[†] Iwan J. P. de Esch,[§] and U. Helena Danielson*[,†,‡]

[†]*Beactica AB, Box 567, SE-751 22 Uppsala, Sweden,* [‡]*Department of Biochemistry and Organic Chemistry, Uppsala University, Box 576, SE-751 23 Uppsala, Sweden, and* [§]*IOTA Pharmaceuticals Ltd. and Division of Medicinal Chemistry, VU University, Amsterdam, The Netherlands*

Received August 13, 2010

A novel scaffold inhibiting wild type and drug resistant variants of human immunodeficiency virus type 1 reverse transcriptase (HIV-1RT) has been identified in a library consisting of 1040 fragments. The fragments were significantly different from already known non-nucleoside reverse transcriptase inhibitors (NNRTIs), as indicated by a Tversky similarity analysis. A screening strategy involving SPR biosensor-based interaction analysis and enzyme inhibition was used. Primary biosensor-based screening, using short concentration series, was followed by analysis of nevirapine competition and enzyme inhibition, thus identifying inhibitory fragments binding to the non-nucleoside reverse transcriptase inhibitor (NNRTI) binding site. Ten hits were discovered, and their affinities and resistance profiles were evaluated with wild type and three drug resistant enzyme variants (K103N, Y181C, and L100I). One fragment exhibited submillimolar K_D and IC_{50} values against all four tested enzyme variants. A substructure comparison between the fragment and 826 structurally diverse published NNRTIs confirmed that the scaffold was novel. The fragment is a bromoindanone with a ligand efficiency of 0.42 kcal/mol^{-1}.

Introduction

The reverse transcriptase of human immunodeficiency virus type 1 (HIV-1[a] RT) is one of the most important targets for the treatment of acquired immunodeficiency syndrome (AIDS).[1] HIV-1 RT is a highly flexible multifunctional enzyme with a heterodimeric structure consisting of a p66 and a p51 subunit. The two subunits have four common subdomains, while the larger p66 subunit has an additional subdomain containing ribonuclease H. Many different classes of HIV-1 RT inhibitors have been described. Two types are usually distinguished on the basis of their mechanism and binding site, with nucleoside reverse transcriptase inhibitors (NRTIs) binding directly to the active site and non-nucleoside reverse transcriptase inhibitors (NNRTIs) binding to an allosteric site, often referred to as the non-nucleoside reverse transcriptase inhibitor binding pocket (NNIBP).[2] Allosteric inhibition of the catalytic function of HIV-1 RT by NNRTIs is primarily considered to be an effect of an induced distortion of the polymerase active site.[3,4] Binding of NNRTIs to the allosteric site also induces considerable restrictions to the conformational flexibility of the enzyme, which has been implied as an additional cause of enzyme inhibition.[5]

Despite the success of HIV-1 RT inhibitors in highly active antiretroviral therapy (HAART), a number of challenges remain.[1] A major problem is that the long-term efficacy of NNRTIs is limited by the rapid emergence of drug-resistant variants of HIV-1.[1] There is hence a continuous need for new lead compounds with lower resistance propensity than current drugs or at least with different resistance profiles. In order to identify novel scaffolds for compounds interfering with the catalysis of HIV-1 RT, a fragment-based[6−9] approach was explored in this study. Two clinically used NNRTIs, nevirapine and delavirdine, and a compound identified in a parallel study[10] were used as references (Figure 1).

A previously developed surface plasmon resonance (SPR) biosensor-based assay for detailed interaction studies of HIV-1 RT with small molecule ligands was used.[11,12] Biosensor-based assays typically cover a wide affinity range, have high information content, low material consumption, and a throughput suitable both for primary screening of fragment libraries and for hit characterization.[8] Because of the low affinity of fragments, high compound concentrations are commonly used for fragment library screening. This can result in signals arising from a number of secondary effects, for example, nonspecific binding (i.e., not well-defined interactions to a single site) and also cause methodological limitations (e.g., carryover, insufficient correction for buffer related signals, and drifting baselines). Hit selection is therefore facilitated when a suitable antitarget (a binding site variant or a closely related target) is available as a reference to compensate for these secondary effects or when a competitor can be used to verify that hits bind to a certain site. For this study, a screening strategy using a stepwise hit selection and validation protocol was developed. It included both an interaction and

*To whom correspondence should be addressed. Address: Department of Biochemistry and Organic chemistry, Uppsala University, Box 576, SE-751 23 Uppsala, Sweden. Phone: +46 18 471 45 45. Fax: +46 18 55 84 31. E-mail: helena.danielson@biorg.uu.se.

[a] Abbreviations: AIDS, acquired immunodeficiency syndrome; FQ, fit quality; HAART, highly active antiretroviral therapy; HIV-1, human immunodeficiency virus type 1; LE, ligand efficiency; MW, molecular weight; NNIBP, non-nucleoside reverse transcriptase inhibitor binding pocket; NRTI, nucleoside reverse transcriptase inhibitor; NNRTI, non-nucleoside reverse transcriptase inhibitor; SPR, surface plasmon resonance; RT, reverse transcriptase; wt, wild type.

Published on Web 01/05/2011

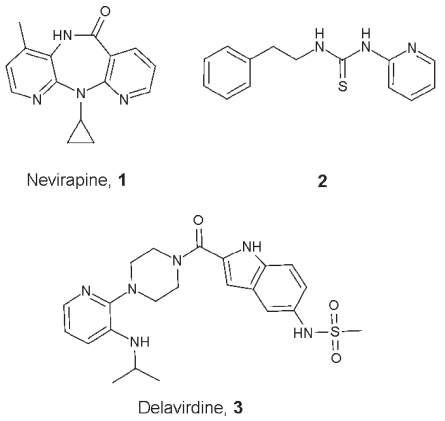

Figure 1. NNRTIs used as reference compounds in screening and hit validation.

an enzyme inhibition assay, similar to the strategy previously successfully implemented for MMP-12.[13] This enabled the identification of fragments binding to the NNIBP and inhibiting both wild type and three drug-resistant variants of the enzyme. It illustrates the applicability of fragment-based screening to the discovery of novel inhibitors of HIV-1 RT despite the challenges recognized for this flexible target whose interaction with NNRTIs is complex. A theoretical analysis of the consequences of such features for fragment hit discovery is outlined in an accompanying study (10.1021/jm101052g).[10]

Results

Potential of Identifying Novel NNRTI Scaffolds in Fragment Library. A Tversky similarity analysis[14] was initially performed to evaluate if the fragment library of interest contained potentially new scaffolds for allosteric inhibitors of HIV-1 RT. The analysis involved a comparison of the 1040 fragments in the library to each of 826 published NNRTIs extracted from the BindingDB.[15] The results showed that 77% of the fragments were less than 70% similar to known NNRTI structures and that 86% were less than 80% similar to known NNRTI structures. Only 28 of the fragments were substructures of known NNRTIs. The molecular weights of these substructures ranged from 85 to 243 Da, with a median value of 155 Da. Although these 28 structures were substructures of NNRTIs in terms of simple atom connectivity, many of them showed an altered functionality and polarity compared to the same structural moiety in the parent NNRTIs. The analysis thus showed that the library was not focused with respect to already known NNRTIs and was therefore considered a promising source for finding novel NNRTIs.

Screening Strategy. Screening of the 1040 compounds was made in three consecutive steps (Figure 2). First the entire library was screened for ligands interacting with wild type HIV-1 RT using a biosensor-based interaction assay (primary screen). The second step consisted of two parallel screens also targeting the wild type enzyme: (A) a biosensor-based competition screen in which the fragments competed with the clinically approved NNRTI nevirapine and (B) an inhibition screen, consisting of an enzyme inhibition assay. Fragments identified as hits in both of these screens were subjected to a third parallel step with further quantification of affinity and inhibition using wild type HIV-1 RT and three drug-resistant enzyme variants (K103N, L100I, Y181C), thereby providing a resistance profile for the fragments.

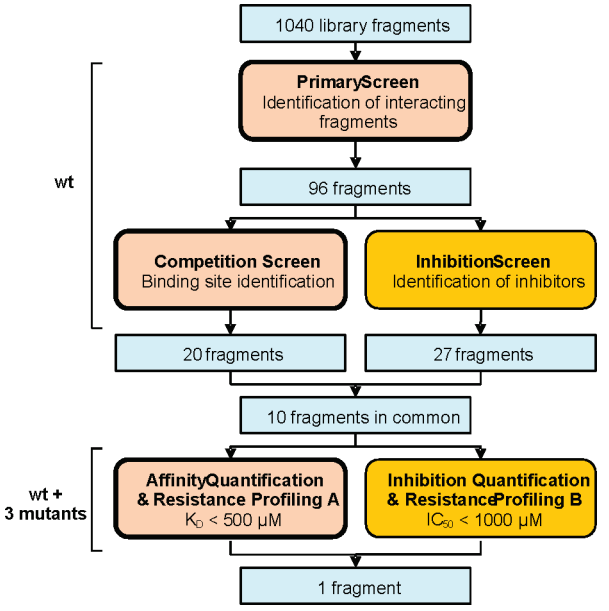

Figure 2. Overview of the screening strategy and the outcome of each step. SPR biosensor experiments are represented by bold rounded boxes (pink), whereas inhibition experiments are represented by thin rounded boxes (orange). The number of fragments used in the different steps and identified as hits in each step are specified in regular boxes (blue).

Primary Screen. A major challenge in fragment library screening is to identify the typically very weak interactions of fragments and to avoid detecting fragments binding promiscuously to the surface or to multiple sites of the target. In order to identify ligands interacting with HIV-1 RT with submillimolar affinity, screening was performed at four fragment concentrations ranging from 50 to 400 μM. Hits were initially identified as fragments that displayed a nonlinear signal vs concentration relationship, i.e., suggestive of a mechanistically simple interaction with a single site. In a first round of the selection process, 165 compounds were selected. These had apparent K_D values of <1 mM and stoichiometries 0.75−5 times the value obtained with the positive control nevirapine.

From this primary selection, further hit triaging was made by visually inspecting whole sets of sensorgrams. This somewhat subjective exercise requires knowledge of the types of signal disturbances that can occur and what their origin is. For instance, the distorted data in Figure 3a are examples of sensorgrams representing fragments of potential interest while the data in Figure 3b show sensorgrams for fragments with undesirable interaction characteristics. By evaluation of basic interaction characteristics such as rate of dissociation, clearance of the biosensor surface, and degree of secondary effects, 69 compounds were eliminated leaving 96 fragments as hits from the primary screen.

Competition and Inhibition Screens. Two independent competition experiments, with 200 μM of each fragment in different compound order and 20 μM nevirapine, were performed with the SPR biosensor. The threshold for the hit selection corresponded approximately to the resolution of the experimental setup; e.g., a fragment with a mass of 150 Da and a K_D of 1 mM could theoretically have been identified as a hit.[16] Sensorgrams of the compounds initially identified as competitors were visually inspected in order to exclude artifacts (as above). Of the 96 hits in the primary screen, 20 were found to compete with nevirapine.

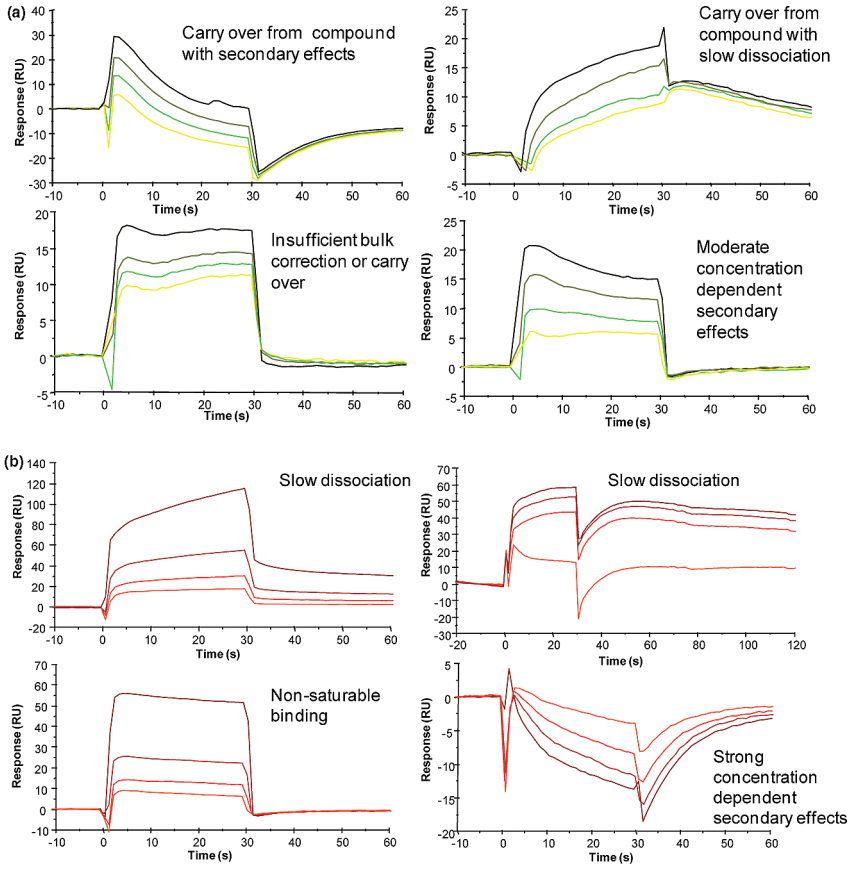

Figure 3. Examples of distorted sensorgrams for fragments (a) accepted as hits and (b) eliminated in the primary screen. The overlay plots represent sensorgrams at fragment concentrations of 50, 100, 200, and 400 μM.

In parallel with the competition screen, the 96 hits from the primary screen were validated also using an enzyme inhibition assay. A set of 27 fragments with IC_{50} values lower than 1 mM were considered as hits. Ten of these were also identified in the competition screen. Consequently, 10 fragments (Figure 4) were thus identified to both compete with nevirapine and inhibit wild type HIV-1 RT with submillimolar IC_{50} values. The identity of all hits was verified, and the purity all compounds was confirmed to be at least 95%.

Affinity Quantification and Interaction-Based Resistance Profiling. The 10 hits common for the competition and inhibition screens were subjected to a more detailed interaction analysis, with the aim to rank the compounds according to estimated affinities (K_D values) for the wild type enzyme (Figure 5) and three drug resistant variants (K103N, Y181C, and L100I), as shown for hit compound **4** in Figure 6.

K_D estimates of fragments within the detectable range are given in Table 1. Two fragments, namely, **4** and **5**, exhibited submillimolar K_D values ($\leq$270 μM) for all four enzyme variants.

Inhibition Quantification and Inhibition-Based Resistance Profiling. IC_{50} values for the 10 hits were redetermined under optimized conditions (Table 1). Compounds were first evaluated against wt HIV-1 RT. Fragments **11** and **12** did not reproducibly show inhibition, indicating that they were false positives in the inhibition screen. These two fragments were hence excluded from further experiments. Inhibition by the eight remaining fragments was further analyzed against three drug-resistant variants of HIV-1 RT (K103N, L100I, Y181C). Four fragments (**4**, **5**, **6**, and **8**) inhibited at least one

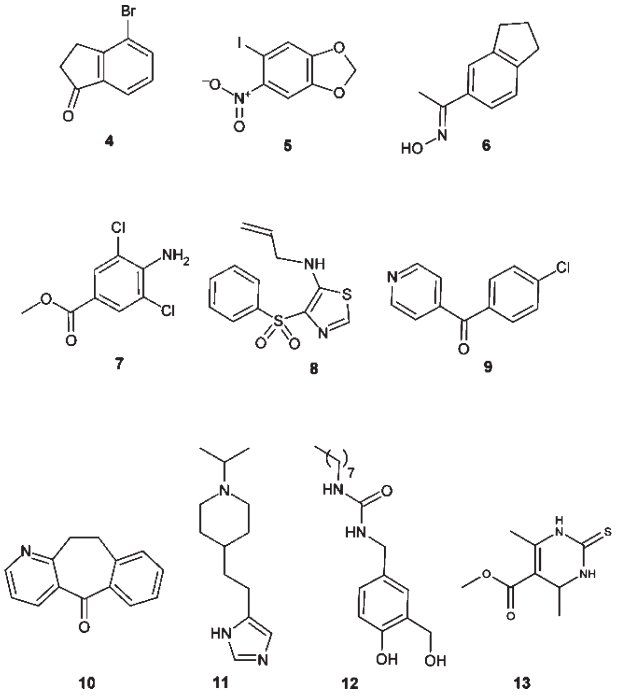

Figure 4. Fragments identified to compete with nevirapine and inhibit wild type HIV-1 RT with submillimolar IC_{50} values.

of the enzyme variants by more than 50% and were therefore reanalyzed in triplicate against the same set of mutants. Fragment **4** was the only fragment that repeatedly showed

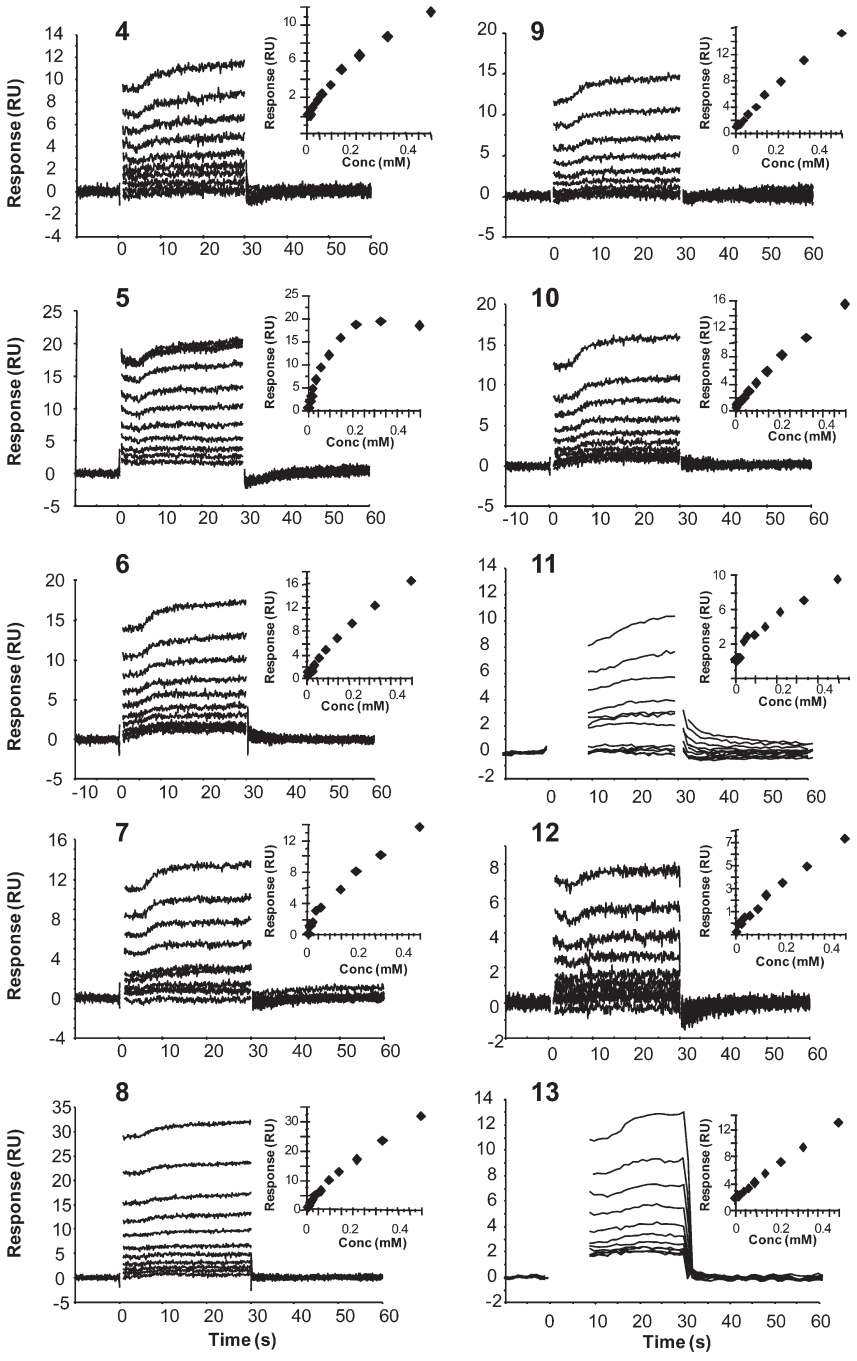

Figure 5. Sensorgrams of the interaction between wt HIV-1 RT and hit compounds in 1.5-fold dilution series from 500 μM.

more than 50% inhibition against all four enzyme variants and that displayed IC_{50} values lower than 25 μM.

Evaluation of Hit Quality. In order to compare the interaction characteristics of the fragments, two types of ligand efficiency parameters were calculated: ligand efficiency (LE)[17] and fit quality (FQ)[18] (see Table 2). These parameters indicate that the interaction between the hits and the target is relatively inefficient. Fragments **4** and **5** showed the highest ligand efficiencies (LE = 0.43−0.44 kcal mol^{-1}), the same LE as for nevirapine. The smaller sizes of **4** and **5** compared to nevirapine would require the ligand efficiency to be significantly higher for conserved fit quality. Thus, the fit quality of fragments **4** and **5** were only 0.47 and 0.50, respectively, which is significantly smaller than for nevirapine (0.63). As a comparison, a prototype ligand with a MW of 500 Da (36 non-hydrogen atoms) and a K_D of 10 nM would have LE = 0.30 kcal mol^{-1} and FQ = 0.76. If fragments **4** and **5** would have bound as efficiently as the prototype ligand, the smallest fragment (i.e., fragment **4**, with 11 non-hydrogen atoms) should have shown an LE of 0.72 kcal mol^{-1}. On the other hand, if the efficiency remains constant throughout lead optimization,[19] the fragments identified in this study would provide excellent starting points. This topic is further discussed and rationalized from a theoretical perspective in the accompanying study (10.1021/jm101052g).[10]

In order to estimate the novelty of the identified scaffolds, a structural similarity analysis for the 20 fragments competing with nevirapine (i.e., disregarding their ability to inhibit the enzyme) and 826 published NNRTIs was also

performed. It showed an average maximum Tversky similarity of 0.55 and a median maximum Tversky similarity of 0.52 (a substructure has a value of 1). This is identical to the average and median for the entire library. These relatively low numbers indicate that the identified hits are structurally novel compared to the 826 NNRTIs used in the comparison. Six of the 28 substructures of known NNRTIs present in the screened fragment library were identified as preliminary hits in the primary screen; however, four of these were eliminated because of slow dissociation (three fragments) or strong secondary effects (one fragment). The remaining two substructures (**14** and **15**, Figure 7) both showed competition with nevirapine in the second screen but failed to inhibit the enzyme. Some examples of NNRTI substructures included in the library are given in Figure 8.

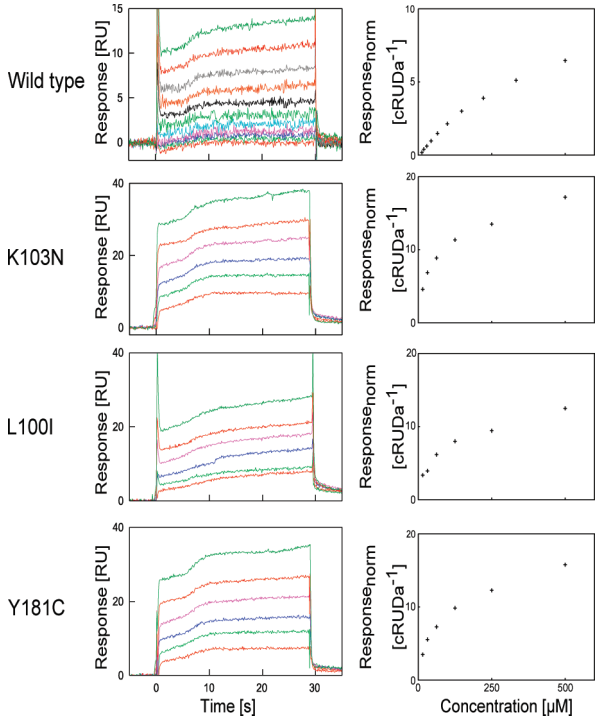

Figure 6. Interaction data for fragment **4** with wild type HIV-1 RT and three drug resistant variants (K103N, L100I, Y181C). Shown are sensorgrams for a series of fragment concentrations up to 500 μM (left). The responses from the sensorgrams were normalized by molecular weight and plotted as a function of concentration (right).

Among the hits shown in Figure 4, fragments **7** and **9** were the most NNRTI-like. They resemble substructures of the published NNRTIs **26** and **27** (Figure 9).[21,25]

Another way to investigate if fragments similar to known NNRTIs are more prone to bind to HIV-1 RT than dissimilar fragments is to create an enrichment plot based on the maximum Tversky similarity. This is done by first sorting the screened fragment library on the basis of maximum Tversky similarity, then plotting the cumulative percent of all hits recovered vs percent of library screened. For this analysis, the 20 fragments found to compete with nevirapine were used as the hit definition. From this standard enrichment plot (Figure 10), it is apparent that the ranking of compounds according to the Tversky similarity is close to a random selection (dotted line). Changing the hit definition to the hits identified in the primary screen did not change these results. Fragments of known NNRTIs were consequently not more frequent among the hits than among the nonhits.

Discussion

The goal of this study was to identify novel scaffolds that allosterically inhibit wild type and drug-resistant variants of HIV-1 RT. Because of the high number of published NNRTIs and the diversity of these structures, this undertaking was a potential challenge. Therefore, prior to the screening, the fragment library was analyzed for diversity against a set of 826 published NNRTIs extracted from the binding database.[15] The Tversky similarity analysis showed that most of the compounds were significantly different from already discovered NNRTIs, indicating a possibility for identification of novel chemistries within the library.

Table 2. Ligand Efficiencies (LE), Fit Qualities (FQ), and Structural Similarities of Fragments Interacting with and Inhibiting HIV-1 RT

compd	n_{HA}	LE (kcal mol^{-1})	FQ	max Tversky similarity
4	11	0.44	0.47	0.62
5	13	0.43	0.50	0.46
6	13	0.37	0.43	0.61
7	13	0.41	0.47	0.80
8	14	0.36	0.43	0.30
9	19	0.22	0.34	0.85
10	16	0.32	0.42	0.43
11	18	0.31	0.45	0.52
12	22	0.23	0.39	0.57
13	17	0.27	0.38	0.30
2[a]	19	0.42	0.63	1.00

[a] Based on K_D = 2 μM for nevirapine (**2**).

Table 1. Affinity (K_D) and Inhibition (IC_{50}) Data for Wild Type (wt) and Drug Resistant HIV-1 RT and Fragments Identified To Compete with Nevirapine and Inhibit Wild Type HIV-1 RT (**4**–**13**)[a]

	wt		K103N		Y181C		L100I	
compd	K_D (μM)[b]	IC_{50} (μM)	K_D (μM)[b]	IC_{50} (μM)	K_D (μM)[b]	IC_{50} (μM)	K_D (μM)[b]	IC_{50} (μM)
4	270	4	20	16	40	16	40	25
5	79	150	20	nd	100	nd	40	nd
6	300	39	50	nd	50	nd	200	nd
7	120	59	200	nd	500	nd	200	nd
8	210	5	700	nd	200	nd	90	nd
9	> 500	96	600	nd	700	nd	60	nd
10	180	430	50	nd	300	nd	200	nd
11	88	nd	nd	–	nd	–	nd	–
12	190	nd	nd	–	nd	–	nd	–
13	380	570	nd	nd	700	nd	nd	nd

[a] Logarithmic values and standard deviations are presented in Supporting Information. nd, no significant binding or inhibition detected. –, not measured. [b] K_D estimated by eq 3.

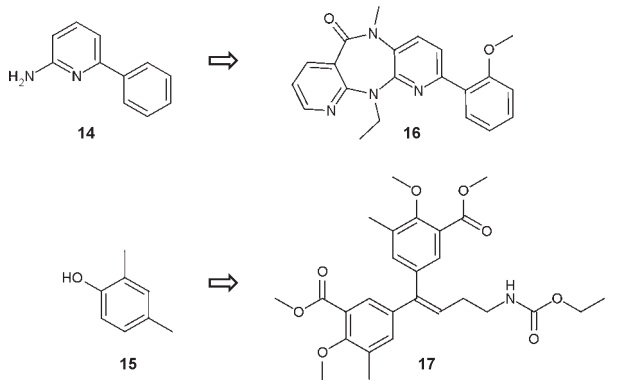

Figure 7. The two fragments that bind to HIV-1 RT and compete with nevirapine but do not inhibit the enzyme (**14** and **15**) represent substructures of published NNRTIs (**16**[20] and **17**[21]).

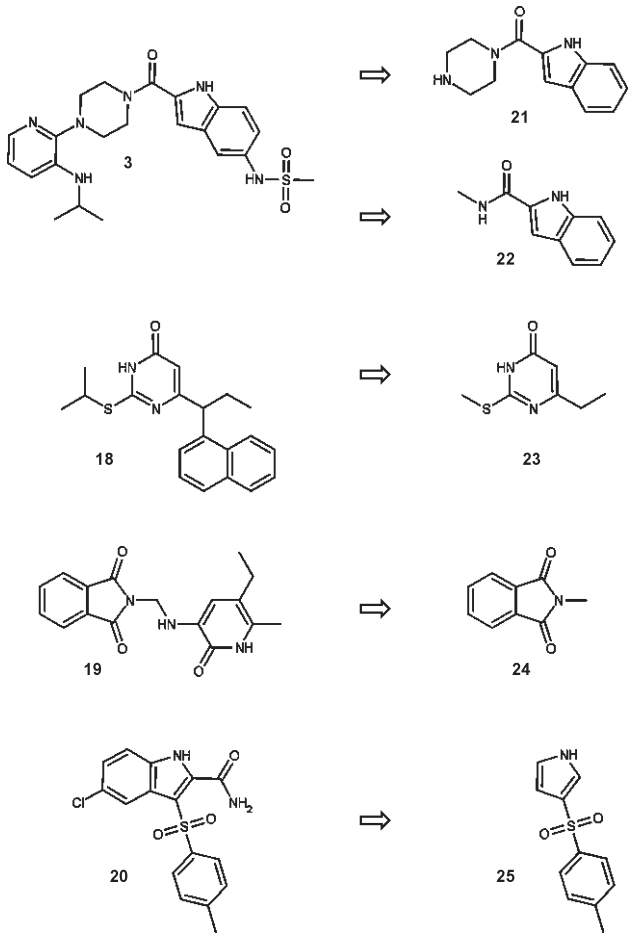

Figure 8. Examples of nonbinding fragments (**21**−**25**) representing substructures of published NNRTIs (**3**, **18**−**20**).[22−24] Compound **3** is delavirdine, one of the reference compounds used.

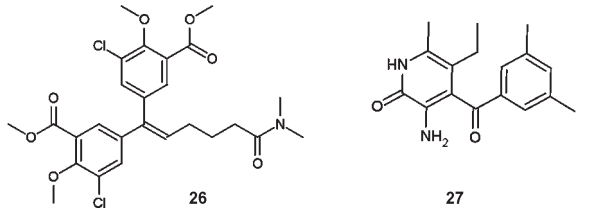

Figure 9. Structures of compounds **26**[21] and **27**,[25] NNRTIs containing substructural elements similar to fragments **7** and **9**.

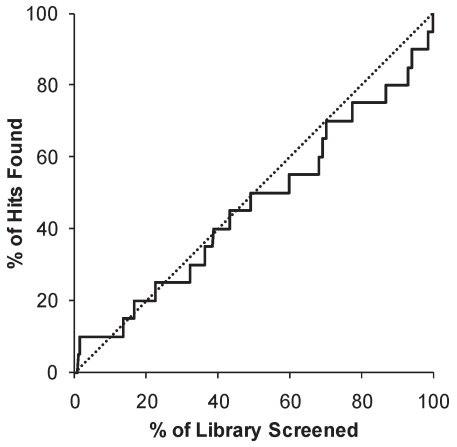

Figure 10. Enrichment curve based on maximum Tversky similarity. An average of random selections is shown as a straight dotted line.

As a result of the weak interactions involved, screening of a fragment library for hits with defined characteristics required a customized experimental strategy that took a multitude of factors into account. The use of multiple concentrations in the initial screen enabled identification of false positives, a potential source of errors due to the label free detection principle and high sensitivity of SPR-based interaction analysis. There are several factors that may change the refractive index close to the sensor surface and thus influence signals and thereby obscure the interpretation of data. For example, poor solubility, conformational changes of the surface bound protein, and unsatisfactory clearance of the biosensor surface (carry over) can give rise to significant effects on signals when screening at high compound concentrations. Fragments giving rise to such secondary effects were detected by visually inspecting the sensorgrams of hits, confirming that a few automatically extracted report points are not reliable for hit selection. The library did not contain a large number of problematic fragments, at least as can be judged from this target. It can therefore be seen as a suitable library for fragment screening using SPR biosensor technology, although we have not subjected it to the same rigorous fragment library validation as another library we have recently designed.[16]

Emphasis in the qualitative analysis was put on the assessment of general interaction characteristics as well as stoichiometry. Fragments displaying slow dissociation and strong secondary effects were eliminated. Removal of compounds exhibiting slow dissociation is a controversial step in SPR-biosensor driven fragment-based drug design (FBDD) and could easily result in false negatives. Nevirapine, with a size of 266 Da and $k_d = 0.01\ s^{-1}$ [10] would, for example, have been rejected in the present screening if it had not been known to be a ligand interacting with the NNIBP. However, fast dissociation was essential for clearance of the biosensor surface after each interaction cycle (no carry over), since no regeneration procedure was available. Therefore, also fast dissociation was used as a hit selection criteria in the primary screen, despite the caveats.

The interaction of fragments with the target was well described by a 1:1 interaction model despite previous evidence for more complex interactions between HIV-1 RT and NNRTIs.[11,26] However, the fragments studied here have significantly weaker affinities for the enzyme, making the interaction less complex. A simple 1:1 model was therefore adequate for the quantification of the kinetic parameters.

The multistep screening strategy involving both interaction and inhibition analysis was similar to a strategy previously used for screening of a fragment library against MMP-12.[13] Here the use of multiple enzyme variants rather than a nontarget was used and competition screening was used only for primary hits. Alternative shortcut strategies for finding new NNRTIs could be devised by replacing the primary screen with a competition screen or with a screen using a blocked NNIBP as a countertarget. An advantage of SPR biosensor based interaction analysis is clearly the possibility of designing the screen and hit validation in a manner where only fragments with certain interaction characteristics will be identified. Still, an orthogonal assay at an early stage is very valuable, as it can detect false positives. The stringent criteria used explain the relatively low hit rate in this study. Relaxing these criteria would obviously increase the "hit rate". Nevertheless, the unexpectedly low hit rate was the basis for the more theoretical analysis and deconstruction of NNRTIs into substructures described in the accompanying paper (10.1021/jm101052g).[10]

The rationale behind the current approach was that the first step identified fragments binding not only to the NNRTI site but also to other sites that may be useful for design of novel inhibitors. This is an interesting option considering the multifunctional characteristics of the enzyme, with the RNase H domain being an additional target for antiviral drug discovery. This multiple approach has already been exploited for the polymerase from hepatitis C virus which has been shown to have several druggable binding sites.[27] By combination of a direct binding screen with a competition screen, it was found that 20 out of 96 primary hits bind to the NNIBP while 76 hits potentially bind to alternative sites. These fragments thus represent interesting starting points for further exploration. However, this was outside the scope of the present study.

The redetermination of the IC_{50} values with the activity based assay under more rigorous conditions turned out to be an important validation step. It showed that 2 of the 10 hits did not inhibit wt HIV-1 RT reproducibly. Moreover, the determination of IC_{50} values showed that high affinity did not warrant a high level of inhibition. This can be explained by the fact that a fragment that binds to an allosteric site with high affinity may not necessarily evoke the conformational change needed for inhibition of the enzymatic activity. Thus, although the IC_{50} values were high, these small fragments could be promising starting points for drug discovery programs. The inhibition assay revealed that no fragments surpassed 75% inhibition. This was also true for nevirapine, which is in line with what previously has been reported for these NNRTIs.[4,28]

Taken together, the interaction and inhibition data suggest that the identified hits bind in the NNIBP, although no structural evidence is yet available. Competition with nevirapine, a molecule that in crystal structures has been shown to bind to the NNIBP of the wild type HIV-1 RT and the three mutants K103N, Y181C, and L100I (Protein Data Bank (PDB) entries 1VRT, 3DRS, 1JLB, and 1S1U), indicates binding to the allosteric pocket. Further support for this hypothesis is the change in IC_{50} and K_D values between the enzyme variants with different amino acid substitutions within the NNIBP (K103N, L100I, and Y181C).

Structural analysis of the 10 hits (Figure 4) showed that the maximum Tversky similarities to the 826 known NNRTIs ranged from 0.30 to 0.85 (Table 2). The similarity analysis is based on the assumption that compounds with similar 2D chemical fingerprints will retain a similarity in the 3D pharmacophore space and that they therefore also should interact likewise with a target protein. It was anticipated that some of the 28 fragments representing substructures of known NNRTIs would have been identified in the screen. Two of these fragments showed up among the 20 hits of the competition screen, but they did not inhibit the enzyme in an enzymatic assay. Thus, substructural similarity to known NNRTIs does not seem to be a predictor of interactions with detectable affinity for the NNIBP, which is also discussed in a parallel paper focusing on the theoretical basis of detection of weakly binding fragments and the importance of binding hot spots.[10] It seems that substructures of known NNRTIs differ in interaction properties from their parent structures, which can be explained by the lack of an efficient binding hot spot within the flexible NNIBP. Polarity and conformational preference of the NNRTI substructures might have changed from that of the parent NNRTIs because of the truncation. This could also partly explain the result that the two hits from the biosensor screen lost their efficacy despite a detectable affinity.

The observed lack of an efficient binding hot spot in HIV-1 RT has implications for the design of fragment-based screens also against other targets with flexible binding sites as well as for the interpretation of screening data (also explored in Brandt et al.[10]). For example, higher screening concentrations may have to be used in order to reach detectable signals. This would result in higher costs and can complicate the data analysis because of a likely increase in secondary effects. We have recently used SPR biosensor-based interaction analysis for identification of ligand efficiency hot spots in acetylcholine binding protein, another system with a flexible ligand binding site.[29]

Since no substructures of NNRTIs were detected as hits in the present screen, it could be argued that the power of fragment-based screening for ligands to flexible binding sites is low. However, identified fragments actually may have the potential to gain superior binding qualities if they can be successfully developed into full-sized ligands. A closer look at the ligand efficiencies (LE) supports this hypothesis; fragment **4** was found to have the highest LE of all molecules with the same number of heavy atoms in the BindingDB. Therefore, compared to previously published fragments, this fragment could represent an excellent starting point for the development of new leads against HIV-1 RT.

A next step would be to perform structure−activity relationship (SAR) studies by investigating properties of structural analogues of fragment **4**, a bromoindanone with few functional groups and no obvious binding mode in the hydrophobic NNIBP. The SPR-based biosensor and enzymatic activity assays employed in the present study are suitable also for such SAR studies. Furthermore, the 17 fragments identified to interact with and inhibit wt HIV-1 RT but not compete with nevirapine for the NNIBP also represent interesting starting points for novel NNRTIs. It is not possible at this stage though to speculate on their mode of action or binding sites.

Conclusion

Despite many challenges in identifying novel scaffolds with a defined mode of action and resistance profile against HIV-1 RT, it is clearly possible to identify novel fragments with desired characteristics in a relatively small library, providing that an efficient experimental design can be used. As exemplified here, one fragment hit was identified in a 1040 compound library. This study, together with a separate analysis of NNRTI

substructures and the theoretical basis of detecting and ranking weakly bound fragments,[10] is expected to contribute to improved design and analysis of fragment-based screens targeting proteins with flexible binding sites.

Experimental Section

Fragment Library. The library consisted of the medicinal chemistry diverse fragment library (1040 fragments) of IOTA Pharmaceuticals Ltd. (Cambridge, U.K.). The fragments had a heavy atoms count of ≤22, log $P < 3$, number of H-bond donors of ≤3, number of H-bond acceptors of ≤3, and number of rotatable bonds mostly of ≤5, with a few exceptions. Gaussian distributions were seen for all parameters except log P where most compounds were found in the 2−3 range (43%) and the 1−2 range (33%).

Verification of Hit Identity and Purity. The identity and purity of the hits (compounds **4**−**13**) were verified by analytical HPLC−MS (OncoTargeting AB, Uppsala, Sweden). An LCMS system consisting of an Agilent 1100 series liquid chromatograph/mass selective detector (Agilent Technologies, Santa Clara, CA, U.S.) was used to obtain the pseudomolecular $[M + H]^+$ ion of the target molecules.

Similarity Analysis. A reference set of 826 HIV-1 RT NNRTI type inhibitors with reported IC_{50} values below 1 μM was extracted from the BindingDB (http://www.bindingdb.org).[15] To assess the novelty of the nevirapine competing fragments discovered in the HIV-1 RT screen and to compare the screened library with known actives, the maximum Tversky similarity between all 826 published HIV-1 RT NNRTI type inhibitors and every compound in the screened fragment library (1040 compounds) was calculated in Canvas (Schrödinger Inc., New York, U.S.). The analysis used 32-bit linear fingerprints based on atomic numbers and bond orders.[30]

Reference Compounds. Two clinically used NNRTIs, nevirapine (**1**) and delavirdine (**3**),[31] were kind gifts from Medivir AB (Huddinge, Sweden). 1-(2-Phenylethyl)-3-pyridin-2-ylthiourea (**2**, Figure 1) was purchased from Vitas-M Laboratory (Moscow, Russia).

Enzyme. Recombinant wild type and drug resistant variants (K103N, Y181C, and L100I) of HIV-1 reverse transcriptase (BH10 isolate) were expressed in *E. coli*, strain BL21 (DE3), and purified as described by Elinder et al.[32] The enzymes had an E478Q substitution in order to abolish the RNase H activity.

Interaction Analysis. Experiments were performed with a Biacore S51 instrument (GE Healthcare Life Sciences, Uppsala, Sweden) at 25 °C. Immobilization of HIV-1 reverse transcriptase was performed essentially as previously described.[11,12] Surface densities between 10 and 15 kRU of HIV-1 RT, prepared by amine coupling to CM5 sensor chips (GE Healthcare Life Sciences, Uppsala, Sweden), were used for the screening and compound characterization.

Primary Screen. All samples were prepared from 40 mM stock solutions as 2-fold dilution series (50−400 μM) in PBS (10 mM phosphate buffer, pH 7.4, 2.7 mM KCl, 0.14 M NaCl) containing 5% DMSO and 0.05% Tween 20. Samples were injected for 30 s at a flow rate of 30 μL/min. As a positive control, 20 μM nevirapine was injected every 24th sample. Subsequent injections of running buffer were used as negative controls. Signals from referenced sensorgrams were typically extracted 4 s before the end of the injections. Alternative time points were chosen when sensorgrams showed disturbances around this time point. Apparent affinities (K_D) and maximal signals (R_{max}) were determined for each compound by a nonlinear fit of the steady-state signals (R) from four ligand concentrations [L] as

$$R = \frac{R_{max}[L]}{[L] + K_D} + m \quad (1)$$

using the Sprint software (Beactica AB, Uppsala, Sweden). The constant m is an offset for each concentration series. Compounds displaying an interaction with an apparent affinity $K_D < 1$ mM and an R_{max} indicating "reasonable stoichiometry" were selected as hits after a visual control of the sensorgrams. Reasonable stoichiometry was defined as an R_{max} higher than $0.75R_{control}$ but lower than $5R_{control}$, the control being 20 μM nevirapine. The values were normalized with respect to molecular weight.

Competition Screen. The same experimental setup as used in the primary screen was used to test the primary hits at single concentrations (200 μM) for competition with 20 μM nevirapine. Two experimental runs with different compound order were performed. Binding levels of fragments interacting with HIV-1 RT were subtracted from binding levels obtained from mixtures of nevirapine and fragments. Fragments resulting in signals that were lower than negative control signals minus 1.8 × standard deviation (SD) in the first experimental run and 3 × SD in the second experimental run were selected.

Inhibition Screening, Quantification, and Resistance Profiling. A catalytic activity assay for HIV-1 RT (Lenti RT Activity Kit, Cavidi AB, Uppsala, Sweden) was used for the inhibition screen, inhibition quantification, and the resistance profiling. Experiments were performed in a 96-well plate format according to "protocol C" provided by the manufacturer. The limiting substrate (poly(A) ribonucleotide template) was present at 200 nM in the final reaction mixture. Colorimetric endpoint detection at a wavelength of 405 nm was conducted using a UV−vis spectrophotometer (SpectraMax, Plus[384], Molecular Devices, Sunnyvale, CA, U.S.).

Activities of wt HIV-1 RT and the three enzyme variants K103N, Y181C, and L100I were assessed by measuring absorbance as a function of enzyme concentration. An enzyme concentration of 2 pM was chosen for the inhibition experiments. Absorbance is directly proportional to enzymatic activity in the applied enzymatic assay. A 1.5-fold dilution series (1.0 μM to 90 nM) was prepared for wt HIV-1 RT and the recombinant HIV-1 RT reference provided with the kit. A 1.5-fold dilution series (1.3 μM to 110 nM) was prepared also for the three RT variants.

In the inhibition screen, inhibition of wt HIV-1 RT was tested at four concentrations (1000, 500, 167, 42 μM). Nevirapine was used as a positive control at four concentrations (40, 20, 7, 2 μM). Each 96-well plate contained fragment samples, blank samples, and standard samples. Blank samples consisted only of the fragment sample reaction mixture (i.e., without fragment or enzyme). The standard samples contained the same reaction mixture plus the enzyme but none of the tested fragments.

Data analysis and determination of IC_{50} values were performed with Excel (Microsoft Corporation, U.S.). Subtraction of the average blank response from all fragment samples and standard samples was performed. The data from the blank corrected fragment samples were normalized by division by the average response of the standard samples.

A global nonlinear regression analysis was applied to determine the three parameters R_{max}, R_{min}, and IC_{50} of the modified Langmuir isotherm (eq 2).Thereby, the parameters R_{max} and R_{min} were determined as global parameters for the data set and an IC_{50} value was determined individually for each compound.

$$R = (R_{max} - R_{min})\left(\frac{IC_{50}}{IC_{50} + [L]}\right) + R_{min} \quad (2)$$

This equation takes into account that full inhibition ($R_{min} = 0$) might not be reached. Starting values for the parameters R_{max} and R_{min} were based on the experimental normalized response values. The starting value for the parameter IC_{50} was set to 100 μM.

The inhibition quantification involved redetermining IC_{50} values in triplicates. Dilution series were designed for each individual fragment so that they had two concentrations below and two concentrations above the preliminary estimate of the IC_{50} values. Nevirapine (40, 20, 7, 2 μM) was included in duplicate. The IC_{50} values were calculated as described above

and subsequently transformed to pIC_{50} values in order to define the error interval on the basis of a linearly scaled data (data shown in Supporting Information). The average of the standard deviation of the pIC_{50} values from each set of triplicates was calculated and transformed back to obtain the final IC_{50} values.

Resistance profiling of hits was performed using three enzyme variants: K103N, Y181C, and L100I. Analysis was based on single measurements at four concentrations (1000, 500, 167, 42 μM), and those showing more than 50% inhibition of at least one of the variants were reanalyzed in triplicate at four compound concentrations (500, 167, 42, 8 μM). Delavirdine was used as a positive control in single measurements at four concentrations (20, 6.6, 1.7, 0.3 μM). Determination of IC_{50} values by global nonlinear regression analysis was performed as described above.

Affinity Quantification and Resistance Profiling. Determination of K_D values was performed with the same experimental setup as used in the primary screen. Immobilization of the enzyme variants (wt HIV-1 RT, variants K103N, L100I, Y181C) on the surface of sensor chip CM5 (GE Healthcare Life Sciences, Uppsala, Sweden) was achieved with enzyme concentrations between 0.3 and 1.0 mg/mL in Hepes buffer. For analyses with wt enzyme, triplicate measurements of each fragment were performed in 1.5-fold dilution series of 11 concentrations (500−9 μM). Compound **2**, used as a positive control, was used to normalize the responses to the decrease in surface activity during each run. Single measurements were performed for the analyses of each fragment with the three mutant variants in 2-fold dilution series (500−15.6 μM). In this case, delavirdine was used as positive control to normalize the responses to the decrease in surface activity during each run. Samples were injected for 30 s at a flow rate of 90 μL/min for wt RT and the three mutants. Injections of running buffer under the same conditions served as negative controls.

The Sprint software (Beactica AB, Uppsala, Sweden) was used for data analysis and determination of K_D values. Reference subtraction and correction for differences in DMSO concentration (solvent correction) were performed with the Biacore software. From each sensorgram a response value was extracted 20 s after the start of the injection. These values were blank subtracted and normalized by division by the molecular weight of the tested compound and thereafter adjusted for surface activity. The parameters R_{max}, m, u, and K_D were determined by a nonlinear regression analysis using eq 3:

$$R = \frac{R_{max}[L]}{[L] + K_D} + u[L] + m \quad (3)$$

The constant u represents a linear unspecific component, including concentration dependent differences in bulk refractive index. The constant m is an offset for each concentration series. A common R_{max} for each separate protein immobilization was fitted using responses from all fragments assayed. The K_D, u, and m were estimated individually for each compound. [L] is the concentration of the ligand (analyte). When fragments were analyzed in replicate, the K_D values were transformed to pK_D values. As for inhibition data, the data were transformed to a linear scale for estimation of errors (see Supporting Information for data). An average pK_D value for each set of replicates was calculated and transformed back to obtain the final K_D value. The standard deviation of the pK_D value from each set of replicates was used to define the error interval.

Calculation of Ligand Efficiency and Fit Quality. Ligand efficiency[17] was calculated by dividing the dissociation free energy by the number of heavy atoms:

$$LE = -RT\ln(K_D)/n_{HA} \quad (4)$$

where n_{HA} is the number of heavy atoms and T is 298 K. The Fit Quality (FQ)[18] was calculated as

$$FQ = -\log(K_D)/[n_{HA}\,LE\,Scale] \quad (5)$$

where

$$LE\ Scale = 0.0715 + 7.53/n_{HA} + 25.7/{n_{HA}}^2 - 361/{n_{HA}}^3 \quad (6)$$

Acknowledgment. Thanks are extended to K. G. Källblad for developing the Sprint software for this project and to Medivir AB for providing the reference NNRTIs nevirapine and delavirdine. This work was supported by a grant from the Seventh Framework Programme of the Commission of the European Communities (Grant HEALTH-F4-2008-202088).

Supporting Information Available: An extended version of Table 1 with logarithmic parameter values and corresponding standard deviations. This material is available free of charge via the Internet at http://pubs.acs.org.

References

(1) Broder, S. The development of antiretroviral therapy and its impact on the HIV-1/AIDS pandemic. *Antiviral Res.* **2010**, *85*, 1–18.
(2) Ren, J.; Stammers, D. K. HIV reverse transcriptase structures: designing new inhibitors and understanding mechanisms of drug resistance. *Trends Pharmacol. Sci.* **2005**, *26*, 4–7.
(3) Ren, J.; Esnouf, R.; Hopkins, A.; Ross, C.; Jones, Y.; Stammers, D.; Stuart, D. The structure of HIV-1 reverse transcriptase complexed with 9-chloro-TIBO: lessons for inhibitor design. *Structure* **1995**, *3*, 915–926.
(4) Spence, R. A.; Kati, W. M.; Anderson, K. S.; Johnson, K. A. Mechanism of inhibition of HIV-1 reverse transcriptase by non-nucleoside inhibitors. *Science* **1995**, *267*, 988–993.
(5) Kohlstaedt, L. A.; Wang, J.; Friedman, J. M.; Rice, P. A.; Steitz, T. A. Crystal structure at 3.5 Å resolution of HIV-1 reverse transcriptase complexed with an inhibitor. *Science* **1992**, *256*, 1783–1790.
(6) Hajduk, P. J.; Greer, J. A decade of fragment-based drug design: strategic advances and lessons learned. *Nat. Rev. Drug Discovery* **2007**, *6*, 211–219.
(7) de Kloe, G. E.; Bailey, D.; Leurs, R.; de Esch, I. J. Transforming fragments into candidates: small becomes big in medicinal chemistry. *Drug Discovery Today* **2009**, *14*, 630–646.
(8) Danielson, U. H. Fragment library screening and lead characterization using SPR biosensors. *Curr. Top. Med. Chem.* **2009**, *9*, 1725–1735.
(9) Danielson, U. H. Integrating surface plasmon resonance biosensor-based interaction kinetic analyses into the lead discovery and optimization process. *Future Med. Chem.* **2009**, *1*, 1399–1414.
(10) Brandt, P.; Geitmann, M.; Danielson, U. H. Deconstruction of non-nucleoside reverse transcriptase inhibitors of human immunodeficiency virus type 1 for exploration of the optimization landscape of fragments. *J. Med. Chem.* DOI: 10.1021/jm101052g.
(11) Geitmann, M.; Unge, T.; Danielson, U. H. Biosensor-based kinetic characterization of the interaction between HIV-1 reverse transcriptase and non-nucleoside inhibitors. *J. Med. Chem.* **2006**, *49*, 2367–2374.
(12) Geitmann, M.; Unge, T.; Danielson, U. H. Interaction kinetic characterization of HIV-1 reverse transcriptase non-nucleoside inhibitor resistance. *J. Med. Chem.* **2006**, *49*, 2375–2387.
(13) Nordström, H.; Gossas, T.; Hämäläinen, M.; Källblad, P.; Nyström, S.; Wallberg, H.; Danielson, U. H. Identification of MMP-12 inhibitors by using biosensor-based screening of a fragment library. *J. Med. Chem.* **2008**, *51*, 3449–3459.
(14) Tversky, A. Features of similarity. *Psychol. Rev.* **1977**, *84*, 327–352.
(15) Liu, T.; Lin, Y.; Wen, X.; Jorissen, R. N.; Gilson, M. K. BindingDB: a web-accessible database of experimentally determined protein−ligand binding affinities. *Nucleic Acids Res.* **2007**, *35*, D198–201.
(16) Elinder, M.; Geitmann, M.; Gossas, T.; Källblad, P.; Winquist, J.; Nordström, H.; Hämäläinen, M.; Danielson, U. H. Experimental validation of a fragment library for lead discovery using SPR biosensor technology. *J. Biomol. Screening*, in press.
(17) Hopkins, A. L.; Groom, C. R.; Alex, A. Ligand efficiency: a useful metric for lead selection. *Drug Discovery Today* **2004**, *9*, 430–431.
(18) Reynolds, C. H.; Bembenek, S. D.; Tounge, B. A. The role of molecular size in ligand efficiency. *Bioorg. Med. Chem. Lett.* **2007**, *17*, 4258–4261.
(19) Hajduk, P. J. Fragment-based drug design: How big is too big? *J. Med. Chem.* **2006**, *49*, 6972–6976.

(20) Proudfoot, J. R.; Hargrave, K. D.; Kapadia, S. R.; Patel, U. R.; Grozinger, K. G.; McNeil, D. W.; Cullen, E.; Cardozo, M.; Tong, L.; Kelly, T. A.; et al. Novel non-nucleoside inhibitors of human immunodeficiency virus type 1 (HIV-1) reverse transcriptase. 4. 2-Substituted dipyridodiazepinones as potent inhibitors of both wild-type and cysteine-181 HIV-1 reverse transcriptase enzymes. *J. Med. Chem.* **1995**, *38*, 4830–4838.

(21) Xu, G.; Micklatcher, M.; Silvestri, M. A.; Hartman, T. L.; Burrier, J.; Osterling, M. C.; Wargo, H.; Turpin, J. A.; Buckheit, R. W., Jr.; Cushman, M. The biological effects of structural variation at the meta position of the aromatic rings and at the end of the alkenyl chain in the alkenyldiarylmethane series of non-nucleoside reverse transcriptase inhibitors. *J. Med. Chem.* **2001**, *44*, 4092–4113.

(22) Mai, A.; Sbardella, G.; Artico, M.; Ragno, R.; Massa, S.; Novellino, E.; Greco, G.; Lavecchia, A.; Musiu, C.; La Colla, M.; Murgioni, C.; La Colla, P.; Loddo, R. Structure-based design, synthesis, and biological evaluation of conformationally restricted novel 2-alkylthio-6-[1-(2,6-difluorophenyl)alkyl]-3,4-dihydro-5-alkylpyrimidin-4(3*H*)-ones as non-nucleoside inhibitors of HIV-1 reverse transcriptase. *J. Med. Chem.* **2001**, *44*, 2544–2554.

(23) Saari, W. S.; Hoffman, J. M.; Wai, J. S.; Fisher, T. E.; Rooney, C. S.; Smith, A. M.; Thomas, C. M.; Goldman, M. E.; O'Brien, J. A.; Nunberg, J. H.; et al. 2-Pyridinone derivatives: a new class of nonnucleoside, HIV-1-specific reverse transcriptase inhibitors. *J. Med. Chem.* **1991**, *34*, 2922–2925.

(24) Silvestri, R.; De Martino, G.; La Regina, G.; Artico, M.; Massa, S.; Vargiu, L.; Mura, M.; Loi, A. G.; Marceddu, T.; La Colla, P. Novel indolyl aryl sulfones active against HIV-1 carrying NNRTI resistance mutations: synthesis and SAR studies. *J. Med. Chem.* **2003**, *46*, 2482–2493.

(25) Dolle, V.; Nguyen, C. H.; Legraverend, M.; Aubertin, A. M.; Kirn, A.; Andreola, M. L.; Ventura, M.; Tarrago-Litvak, L.; Bisagni, E. Synthesis and antiviral activity of 4-benzyl pyridinone derivatives as potent and selective non-nucleoside human immunodeficiency virus type 1 reverse transcriptase inhibitors. *J. Med. Chem.* **2000**, *43*, 3949–3962.

(26) Elinder, M.; Selhorst, P.; Vanham, G.; Öberg, B.; Vrang, L.; Danielson, U. Inhibition of HIV-1 by non-nucleoside reverse transcriptase inhibitors via an induced fit mechanism. Importance of slow dissociation and relaxation rates for antiviral efficacy. *Biochem. Pharmacol.* **2010**, *80*, 1133–1140.

(27) Kwong, A. D.; McNair, L.; Jacobson, I.; George, S. Recent progress in the development of selected hepatitis C virus NS3.4A protease and NS5B polymerase inhibitors. *Curr. Opin. Pharmacol.* **2008**, *8*, 522–531.

(28) Xia, Q.; Radzio, J.; Anderson, K. S.; Sluis-Cremer, N. Probing nonnucleoside inhibitor-induced active-site distortion in HIV-1 reverse transcriptase by transient kinetic analyses. *Protein Sci.* **2007**, *16*, 1728–1737.

(29) de Kloe, G. E.; Retra, K.; Geitmann, M.; Källblad, P.; Smit, A. B.; van Muijlwijk-Koezen, J. E.; Leurs, R.; Irth, H.; Danielson, U. H.; De Esch, I. J. P. Surface plasmon resonance biosensor based fragment screening using acetylcholine binding protein identifies ligand efficiency hot spots (LE hot spots) by deconstruction of nicotinic acetylcholine receptor alpha7 ligands. *J. Med. Chem.* **2010**, *53*, 7192–7201.

(30) Sastry, M.; Lowrie, J. F.; Dixon, S. L.; Sherman, W. Large-scale systematic analysis of 2D fingerprint methods and parameters to improve virtual screening enrichments. *J. Chem. Inf. Model.* **2010**, *50*, 771–784.

(31) de Bethune, M. P. Non-nucleoside reverse transcriptase inhibitors (NNRTIs), their discovery, development, and use in the treatment of HIV-1 infection: a review of the last 20 years (1989−2009). *Antiviral Res.* **2010**, *85*, 75–90.

(32) Elinder, M.; Nordström, H.; Geitmann, M.; Hämäläinen, M.; Vrang, L.; Öberg, B.; Danielson, U. H. Screening for NNRTIs with slow dissociation and high affinity for a panel of HIV-1 RT variants. *J. Biomol. Screening* **2009**, *14*, 395–403.